JCTC Journal of Chemical Theory and Computation

Letter

pubs.acs.org/JCTC

Development of a "First-Principles" Water Potential with Flexible Monomers. III. Liquid Phase Properties

Gregory R. Medders,[†] Volodymyr Babin,[†] and Francesco Paesani*

Department of Chemistry and Biochemistry, University of California, San Diego, La Jolla, California 92093, United States

ABSTRACT: The MB-pol full-dimensional water potential introduced in the first two papers of this series [*J. Chem. Theory Comput.* **2013**, *9*, 5395 and *J. Chem. Theory Comput.* **2014**, *10*, 1599] is employed here in classical and quantum simulations of liquid water under ambient conditions. Comparisons with the available experimental data for several structural, thermodynamic, and dynamical properties indicate that MB-pol provides a highly accurate description of the liquid phase. Combined with previous analyses of the dimer vibration−rotation tunneling spectrum, second and third virial coefficients, and cluster structures and energies, the present results demonstrate that MB-pol represents a major step toward the long-sought "universal model" capable of describing the properties of water from the gas to the condensed phases.

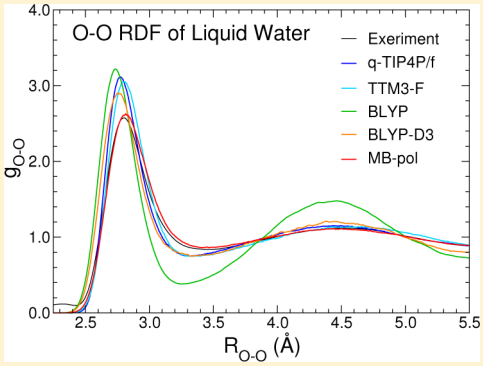

The accurate representation of intermolecular interactions combined with the development and implementation of efficient theoretical/computational approaches for simulations of large molecular systems still remain challenging problems in electronic structure theory. In many respects, these two problems are incompatible with each other because the accurate calculation of noncovalent interactions typically requires the use of highly correlated methods whose associated computational cost effectively precludes their application to large systems. As a result, despite significant recent progress, chemical accuracy remains out of reach for most simulations of condensed phase systems.[1−11] This is well exemplified by the plethora of water potentials that have been developed over the years (including both force fields with different degrees of empiricism and *ab initio* models), none of which, however, is capable of correctly describing the properties of water from isolated molecules and small clusters in the gas phase to the bulk phases (e.g., see refs 12−16).

Recent studies have demonstrated that the many-body expansion of the interaction energy[17] converges rapidly for water,[18−25] providing a rigorous approach for the development of accurate multidimensional potential energy surfaces (PESs) for water systems of arbitrary sizes. This rapid convergence of the many-body expansion has previously been exploited by *ab initio*-based interaction potentials, which enable a rigorous treatment of the many-body expansion of interactions through a functional form that is sufficiently flexible to accurately capture the complexity of high-quality *ab initio* reference data. Examples of such models are DPP2,[26] CC-pol,[27] WHBB,[28] and our previous water potential, HBB2-pol.[29,30] In the first two papers of this series,[14,16] we have introduced the MB-pol potential that, building on the many-body formalism and the HBB2-pol model, expresses the total energy of a system containing N water molecules as

$$E_N(x_1, ..., x_N) = \sum_a V^{(1B)}(x_a) + \sum_{a>b} V^{(2B)}(x_a, x_b) + \sum_{a>b>c} V^{(3B)}(x_a, x_b, x_c) + V^{(MB)}(x_1, ..., x_N) \quad (1)$$

Here, x_a denotes the coordinates of all atoms in the ath molecule and $V^{(nB)}$ are the n-body interactions defined recursively as

$$V^{(nB)}(x_1, ..., x_n) = E_n(x_1, ..., x_n) - \sum_a V^{(1B)}(x_a) - \sum_{a>b} V^{(2B)}(x_a, x_b) - ... - \sum_{a_1>a_2>...>a_{n-1}} V^{((n-1)B)}(x_{a_1}, x_{a_2}, ..., x_{a_{n-1}}) \quad (2)$$

In the MB-pol energy expression, the one-body term, $V^{(1B)}$, is associated with the intramolecular distortion of each water molecule and is described by the spectroscopically accurate monomer PES developed by Partridge and Schwenke.[31] The two-body term, $V^{(2B)}$, is split into short- and long-range contributions:

$$V^{(2B)}(x_a, x_b) = V^{(2B)}_{short}(x_a, x_b) + V^{(2B)}_{long}(x_a, x_b) \quad (3)$$

The short-range component, $V^{(2B)}_{short}(x_a, x_b)$, is represented by a permutationally invariant polynomial that smoothly switches to zero once the separation between two water molecules becomes larger than a predetermined cutoff value. The long-range component, $V^{(2B)}_{long}(x_a, x_b)$, is instead represented by electrostatic contributions arising from interactions between permanent and induced moments associated with the molecular

Received: May 12, 2014

   dx.doi.org/10.1021/ct5004115 | *J. Chem. Theory Comput.* XXXX, XXX, XXX−XXX

charge distributions as well as by dispersion forces.[14] The MB-pol 3-body term, $V^{(3B)}$, takes the form

$$V^{(3B)}(x_a, x_b, x_c) = V^{(3B)}_{short}(x_a, x_b, x_c) + V^{(3B)}_{ind}(x_a, x_b, x_c) \quad (4)$$

where $V^{(3B)}_{ind}$ represents the three-body induction energy, and $V^{(3B)}_{short}$ is a short-range permutationally invariant polynomial.[16] All n-body terms with $n \geq 4$ are described through many-body induction interactions represented by the $V^{(MB)}(x_1,...,x_N)$ term in eq 1. Both the two-body and three-body terms of the MB-pol potential were derived from highly accurate fits to the corresponding *ab initio* energies calculated at the CCSD(T)/CBS and CCSD(T)/aug-cc-pVTZ levels of theory, respectively, imposing the correct asymptotic behavior as predicted from "first-principles."[14,16] The induction contributions to the n-body energies are modeled using the same Thole-type scheme[32] adopted by the TTM4-F model[33] with a slight modification as described in ref 14. The accuracy of the MB-pol potential in reproducing the properties of finite-size water systems was assessed in refs 14 and 16 through a detailed analysis of the dimer vibration−rotation tunneling spectrum, second and third virial coefficients, and cluster structures and energies. In this Letter we report on classical and quantum dynamics simulations carried out with the MB-pol potential for liquid water under ambient conditions. Direct comparison with the corresponding experimental data demonstrates the ability (so far unique among the existing water models) of the MB-pol potential of correctly predicting the water properties from the dimer to the liquid phase entirely from "first-principles."

Since the MB-pol potential provides an accurate representation of the multidimensional Born−Oppenheimer PES for water,[14,16] it must be combined with simulation approaches that explicitly take into account nuclear quantum effects for a truly "first-principles" description of bulk properties. In this study, path-integral molecular dynamics (PIMD)[34−37] and centroid molecular dynamics (CMD)[38] are used to calculate structural, thermodynamic, and dynamical properties of liquid water at T = 298.15 K and P = 1 atm. Since both methods and recent applications to aqueous systems have been reviewed recently,[39] only a brief summary of the main concepts is given here. PIMD is based on Feynman's formulation of statistical mechanics in terms of path integrals[40] and exploits the isomorphism between the quantum partition function of a system of N particles and the classical partition function of a system consisting of N flexible ring polymers.[34] By construction, PIMD enables the calculation of numerically exact structural and thermodynamic properties of quantum-mechanical systems.[41] The CMD formalism draws upon the prescription of distribution functions in which the exact quantum expressions are cast into a convenient phase space representation of the system dynamics.[42−48] The latter is described by classical-like equations of motion applied to the centroid coordinates corresponding to the centers of mass of the ring polymers that represent the quantum particles within the path-integral formalism. The CMD time propagation thus enables the calculation of quantum time correlation functions that can then be used to characterize the properties of condensed-phase systems within linear response theory.[49]

All simulations discussed in the following were carried out for a system consisting of 256 H_2O molecules in a periodic cubic box. Each atom was represented by a ring polymer with P = 32 beads. For comparison, simulations with a single bead (P = 1) were also performed to model the properties of water at the classical level. The PIMD simulations were carried out using the normal mode representation of the ring polymers,[37] which enables an efficient sampling of the quantum partition function.[50] All PIMD simulations were carried out in both constant temperature−constant volume (NVT) and constant temperature−constant pressure (NPT) ensembles. The equations of motion were propagated using the velocity-Verlet algorithm with a time step Δt = 0.2 fs. The temperature was controlled via Nosé−Hoover chains (NHC) of four thermostats coupled to each degree of freedom.[51] The NPT ensemble was generated according to the algorithm described in ref 52.

In the CMD simulations, the centroid force was computed "on the fly" exploiting the time-scale separation between the dynamics of the centroid degrees of freedom and the nonzero frequency normal modes.[45] The propagation of the centroid variables was carried out in the constant energy−constant volume (NVE) ensemble with NHC of four thermostats attached to each nonzero frequency normal mode. An adiabaticity parameter γ = 0.1 and a time step Δt = 0.025 fs ensured a sufficiently large separation in time between the motion of the centroid and the nonzero frequency normal modes as well as a proper integration of the latter. In both PIMD and CMD simulations, a radial atom−atom cutoff distance of 9.0 Å was applied to the nonbonded interactions and the Ewald sum was used to treat the long-range electrostatic interactions.[53] The structural and thermodynamic properties were obtained by averaging over 1-ns-long PIMD simulations in the NPT ensemble and a 100 ps simulation in NVT. The dynamic properties were obtained by averaging over 10 independent CMD trajectories of 10 ps each. For the classical NVE simulations, two independent 200 ps simulations were performed due to the relatively long lifetime of the orientational correlation function in the classical case.

The thermodynamic properties of liquid water under ambient conditions as predicted by the MB-pol potential are first analyzed. A comparison between the classical and quantum results along with the corresponding experimental data for the liquid density and enthalpy of vaporization is reported in Table 1. The density predicted by the PIMD simulations is appreciably smaller than its classical counterpart and in closer agreement with the experimental value. As discussed in previous studies (e.g., see ref 54), the explicit quantization of the nuclear motion results in an increase of the molecular dimensions due to zero-point energy effects and delocalization, which are thus responsible for the relatively lower density of the liquid at the quantum-mechanical level. Both classical and

Table 1. Thermodynamic and Dynamical Properties of Liquid Water at Ambient Conditions As Predicted by Classical and Quantum Simulations with the MB-pol Potential[a]

	density (g cm^{-3})	H_{vap} (kcal mol^{-1})	τ_2 (ps)	D (Å^2 ps^{-1})
classical	1.004(1)	10.9(2)	5.3(2)	0.12(1)
quantum	1.001(2)	10.1(4)	2.3(3)	0.22(3)
experiment	0.997[(a)]	10.5176[(b)]	2.5[(c)]	0.23[(d)]

[a]Both density (ρ) and enthalpy of vaporization (H_{vap}) were calculated in the NPT ensemble, while the orientational relaxation time (τ_2) and diffusion constant (D) were calculated in the NVE ensemble. Experimental data: (a) from ref 55, (b) from ref 56, (c) from ref 57, and (d) from ref 58.

dx.doi.org/10.1021/ct5004115 | J. Chem. Theory Comput. XXXX, XXX, XXX−XXX

quantum results for the enthalpy of vaporization are in similar agreement with the corresponding experimental value.

The differential neutron scattering cross sections per atom calculated from NPT simulations carried out at both classical and quantum levels are shown in Figure 1 along with the

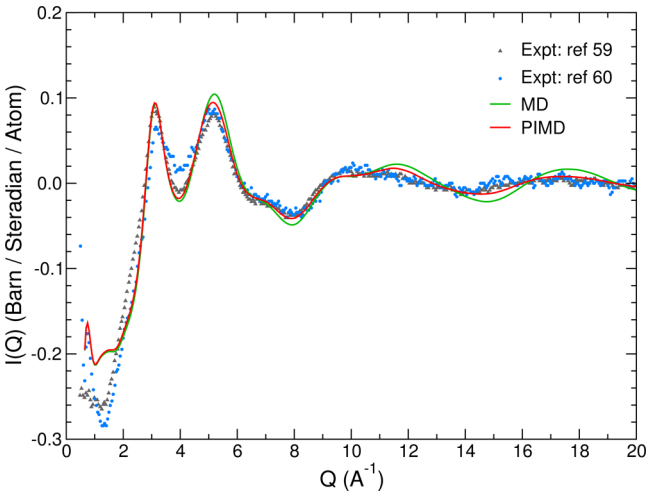

Figure 1. Differential neutron scattering cross-section per atom calculated from classical (MD, green) and quantum (PIMD, red) simulations of liquid water at T = 298.15 K and P = 1 atm. The experimental data are taken from ref 59 (gray) and from ref 60 (light blue).

available experimental data.[59,60] This comparison demonstrates that PIMD simulations with the MB-pol potential accurately represent liquid water under ambient conditions. The difference between classical and quantum results also indicate the presence of non-negligible nuclear quantum effects on the liquid structure as already discussed in the literature (e.g., see ref 39 for a recent review).

Classical and quantum oxygen−oxygen (O−O), oxygen−hydrogen (O−H), and hydrogen−hydrogen (H−H) radial distribution functions (RDFs) calculated in the NPT ensemble are compared in Figure 2 with three recent sets of experimental data.[59−61] As expected from the analysis of the differential neutron scattering cross-section, the PIMD O−O RDF correctly reproduces the experimental results, predicting a relatively lower first peak compared with estimates obtained from simulations with common force fields and DFT models (see Figure 3). As already observed for the HBB2-pol[29] and TTM3-F[62] potentials, some differences between MB-pol and experimental results exist for the second peak of the O−H RDF. In this regard, it is important to note that both the position and shape of this peak, which describes the spatial correlation between O and H atoms directly involved in hydrogen bonds, are difficult to determine experimentally as demonstrated by the appreciable differences between the two sets of experimental data.

To test the ability of different water models (with flexible monomers) to reproduce the experimentally derived O−O RDFs, both classical and quantum O−O RDFs of q-TIP4P/f,[63] TTM3-F,[62] BLYP,[64] and BLYP-D3[65,66] were compared against the most recent experiments and MB-pol in Figure 3. These three models, whose ability to describe the many-body energies was assessed in ref 30, were chosen as representative of fixed-charge, polarizable, and DFT potentials that are commonly used in quantum simulations of liquid water. From the

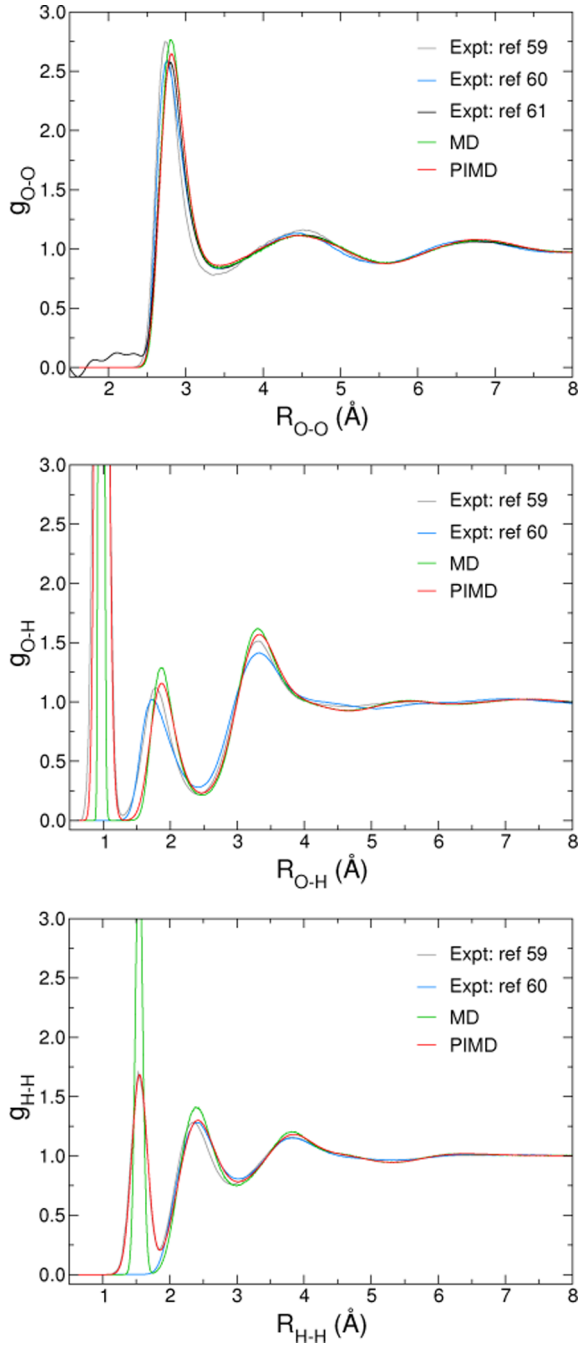

Figure 2. O−O, O−H, and H−H RDFs calculated from both classical (MD, green) and quantum (PIMD, red) NPT simulations with the MB-pol potential at T = 298.15 K and P = 1 atm compared with the corresponding experimental data from ref 59 (gray), from ref 60 (light blue), and from ref 61 (black).

comparison shown in Figure 3, q-TIP4P/f, TTM3-F, BLYP, and BLYP-D3 predict an overstructured first solvation shell, which is particularly evident in the case of BLYP. Among these four water models, BLYP-D3 is in relatively better agreement with the experimental data, displaying a slightly lower first peak in the O−O RDF than q-TIP4P/f and TTM3-F. As mentioned above, similar deficiencies are common to the majority of water models reported in the literature. A notable exception are the results obtained with the CC-pol potential, which, however, neglects intramolecular flexibility.[27]

dx.doi.org/10.1021/ct5004115 | J. Chem. Theory Comput. XXXX, XXX, XXX−XXX

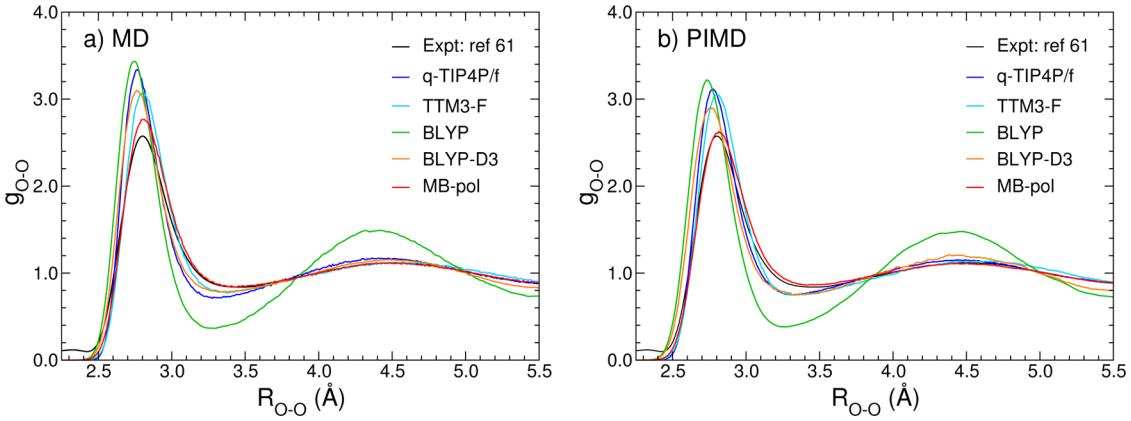

Figure 3. Comparsion between classical (panel a, MD) and quantum (panel b, PIMD) O−O RDF obtained from NVT simulations at the experimental density carried out at T = 298.15 K with the q-TIP4P/f (blue), TTM3-F (cyan), BLYP (green), BLYP-D3 (orange), and MB-pol (red) potentials. The BLYP and BLYP-D3 results are taken from simulations carried out at 300 K in refs 64 and 66, respectively. The experimental results (black) are from ref 61.

The diffusion coefficient (D) and orientational relaxation time (τ_2) calculated at both classial and quantum levels are listed in Table 1. The diffusion constant was calculated from integration of the velocity autocorrelation function:[53]

$$D = \frac{1}{3}\int_0^\infty \langle v(0)\cdot v(t)\rangle \tag{5}$$

The orientational relaxation time was obtained by fitting the long-time decay of the time autocorrelation function of the second-order Legendre polynomial, C_2 (t) in eq 6, to a single exponential.

$$C_2(t) = \langle P_2[e(0)\cdot e(t)]\rangle \tag{6}$$

In eq 6, $e(t)$ is a unit vector along each OH bond in the body-fixed reference frame of the corresponding water molecule. The quantum results were obtained by averaging over 10 CMD trajectories of 10 ps each, while the classical results were calculated using two NVE trajectories of 200 ps. For both quantities, the CMD results are in quantitative agreement with the corresponding experimental values, providing further evidence of the accuracy of the MB-pol model. Interestingly, the differences between classical and quantum results are significantly larger than estimates recently reported with the q-TIP4P/f potential.[63] This difference suggests that the effects of nuclear quantization on the water properties are nontrivial even under ambient conditions and are particularly sensitive to the accuracy of the underlying PES.

In summary, the full-dimensional MB-pol potential introduced in refs 14 and 16 has been employed in classical and quantum simulations of liquid water under ambient conditions. The agreement between the simulation predictions and the experimental data indicates that MB-pol represents a major step toward the long-sought "universal model" capable of describing the behavior of water under different conditions and in different environments.[67] In this context, the MB-pol potential appears to be well suited for a fully "first-principles" characterization of the pressure−temperature properties of water, which may help resolve some of the current controversies regarding structural, thermodynamic, and dynamical properties of bulk, interfacial, and supercooled water.

AUTHOR INFORMATION

Corresponding Author

*E-mail: fpaesani@ucsd.edu.

Author Contributions

†Contributed equally to this work.

Notes

The authors declare no competing financial interest.

ACKNOWLEDGMENTS

This research was supported by the National Science Foundation Center for Chemical Innovation "Center for Aerosol Impacts on Climate and the Environment" (grant CHE-1305427). We are grateful to Prof. Michele Ceriotti for providing the classical and quantum O−O RDFs calculated with BLYP in ref 64 as well as the corresponding results obtained with BLYP-D3.

REFERENCES

(1) Car, R.; Parrinello, M. *Phys. Rev. Lett.* **1985**, *55*, 2471−2474.
(2) Xie, W.; Song, L.; Truhlar, D. G.; Gao, J. *J. Chem. Phys.* **2008**, *128*, 234108.
(3) Gordon, M. S.; Slipchenko, L.; Li, H.; Jensen, J. H. *Annu. Rep. Comput. Chem.* **2007**, *3*, 177−193.
(4) Chang, D. T.; Schenter, G. K.; Garrett, B. C. *J. Chem. Phys.* **2008**, *128*, 164111.
(5) Murdachaew, G.; Mundy, C. J.; Schenter, G. K.; Laino, T.; Hutter, J. *J. Phys. Chem. A* **2011**, *115*, 6046−6053.
(6) Del Ben, M.; Schönherr, M.; Hutter, J.; VandeVondele, J. *J. Phys. Chem. Lett.* **2013**, *4*, 3753−3759.
(7) Bartók, A. P.; Gillan, M. J.; Manby, F. R.; Csányi, G. *Phys. Rev. B* **2013**, *88*, 054104.
(8) Wen, S.; Beran, G. J. O. *J. Chem. Theory Comput.* **2011**, *7*, 3733−3742.
(9) Zhang, C.; Wu, J.; Galli, G.; Gygi, F. *J. Chem. Theory Comput.* **2011**, *7*, 3054−3061.
(10) Richard, R. M.; Herbert, J. M. *J. Chem. Phys.* **2012**, *137*, 064113.
(11) Morales, M. A.; Gergely, J. R.; McMinis, J.; McMahon, J. M.; Kim, J.; Ceperley, D. M. *J. Chem. Theory Comput.* **2014**, *10*, 2355−2362.
(12) Vega, C.; Abascal, J. L. F. *Phys. Chem. Chem. Phys.* **2011**, *13*, 19663−19688.
(13) Møgelhøj, A.; Kelkkanen, A. K.; Wikfeldt, K. T.; Schiøtz, J.; Mortensen, J. J.; Pettersson, L. G. M.; Lundqvist, B. I.; Jacobsen, K. W.; Nilsson, A.; Nørskov, J. K. *J. Phys. Chem. B* **2011**, *115*, 14149−60.

(14) Babin, V.; Leforestier, C.; Paesani, F. *J. Chem. Theory Comput.* **2013**, *9*, 5395−5403.
(15) Babin, V.; Paesani, F. *Chem. Phys. Lett.* **2013**, *580*, 1−8.
(16) Babin, V.; Medders, G. R.; Paesani, F. *J. Chem. Theory Comput.* **2014**, *10*, 1599−1607.
(17) Mayer, J. E.; Mayer, M. G. *Statistical Mechanics*; John Wiley & Sons Inc.: Hoboken, NJ, 1940.
(18) Xantheas, S. S. *J. Chem. Phys.* **1994**, *100*, 7523−7534.
(19) Pedulla, J. M.; Vila, F.; Jordan, K. D. *J. Chem. Phys.* **1996**, *105*, 11091.
(20) Hodges, M. P.; Stone, A. J.; Xantheas, S. S. *J. Phys. Chem. A* **1997**, *101*, 9163−9168.
(21) Xantheas, S. S. *Chem. Phys.* **2000**, *258*, 225−231.
(22) Cui, J.; Liu, H. B.; Jordan, K. D. *J. Phys. Chem. B* **2006**, *110*, 18872−18878.
(23) Hermann, A.; Krawczyk, R.; Lein, M.; Schwerdtfeger, P.; Hamilton, I.; Stewart, J. J. P. *Phys. Rev. A* **2007**, *76*, 013202.
(24) Góra, U.; Podeszwa, R.; Cencek, W.; Szalewicz, K. *J. Chem. Phys.* **2011**, *135*, 224102.
(25) Khaliullin, R. Z.; Cobar, E. A.; Lochan, R. C.; Bell, A. T.; Head-Gordon, M. *Phys. Chem. Chem. Phys.* **2012**, *14*, 15328−15339.
(26) Kumar, R.; Wang, F.; Jenness, G. R.; Jordan, K. D. *J. Chem. Phys.* **2010**, *132*, 014309.
(27) Bukowski, R.; Szalewicz, K.; Groenenboom, G. C.; van der Avoird, A. *Science* **2007**, *315*, 1249−52.
(28) Wang, Y.; Huang, X.; Shepler, B. C.; Braams, B. J.; Bowman, J. M. *J. Chem. Phys.* **2011**, *134*, 094509.
(29) Babin, V.; Medders, G. R.; Paesani, F. *J. Phys. Chem. Lett.* **2012**, *3*, 3765−3769.
(30) Medders, G. R.; Babin, V.; Paesani, F. *J. Chem. Theory Comput.* **2013**, *9*, 1103−1114.
(31) Partridge, H.; Schwenke, D. W. *J. Chem. Phys.* **1997**, *106*, 4618.
(32) Thole, B. T. *Chem. Phys.* **1981**, *59*, 341−350.
(33) Burnham, C. J.; Hayashi, T.; Napoleon, R. L.; Keyes, T.; Mukamel, S.; Reiter, G. F. *J. Chem. Phys.* **2011**, *135*, 144502.
(34) Chandler, D.; Wolynes, P. G. *J. Chem. Phys.* **1981**, *74*, 4078−4095.
(35) Parrinello, M.; Rahman, A. *J. Chem. Phys.* **1984**, *80*, 860−867.
(36) De Raedt, B.; Sprik, M.; Klein, M. L. *J. Chem. Phys.* **1984**, *80*, 5719−5724.
(37) Berne, B. J.; Thirumalai, D. *Annu. Rev. Phys. Chem.* **1986**, *37*, 401−424.
(38) Voth, G. A. *Adv. Chem. Phys.* **1996**, *93*, 135.
(39) Paesani, F.; Voth, G. A. *J. Phys. Chem. B* **2009**, *113*, 5702−19.
(40) Feynman, R. P. *Statistical Mechanics*; Benjamin: New York, 1972.
(41) Tuckerman, M. In *Quantum Simulations of Complex Many-Body Systems: From Theory to Algorithms*; Grotendorst, J., Marx, D., Muramatsu, A., Eds.; John von Neumann Institute for Computing: Jülich, Germany, 2002; Vol. *10*; pp 269−298.
(42) Cao, J.; Voth, G. A. *J. Chem. Phys.* **1994**, *100*, 5093−5105.
(43) Cao, J.; Voth, G. A. *J. Chem. Phys.* **1994**, *100*, 5106−51117.
(44) Cao, J.; Voth, G. A. *J. Chem. Phys.* **1994**, *101*, 6157−6167.
(45) Cao, J.; Voth, G. A. *J. Chem. Phys.* **1994**, *101*, 6168−6183.
(46) Cao, J.; Voth, G. A. *J. Chem. Phys.* **1994**, *101*, 6184−6192.
(47) Jang, S.; Voth, G. A. *J. Chem. Phys.* **1999**, *111*, 2357−2370.
(48) Jang, S.; Voth, G. A. *J. Chem. Phys.* **1999**, *111*, 2371−2384.
(49) Berne, B. J.; Harp, G. D. In *Advances in Chemical Physics*; Prigogine, I., Rice, S., Eds.; John Wiley & Sons: Hoboken, NJ, 1970; pp 63−227.
(50) Hall, W. R.; Berne, B. J. *J. Chem. Phys.* **1984**, *81*, 3641.
(51) Martyna, G. J.; Klein, M. L.; Tuckerman, M. E. *J. Chem. Phys.* **1992**, *97*, 2635−2643.
(52) Martyna, G. J.; Hughes, A.; Tuckerman, M. E. *J. Chem. Phys.* **1999**, *110*, 3275.
(53) Allen, M. P.; Tildesley, D. J. *Computer Simulations of Liquids*; Clarendon Press: Oxford, U. K., 1987.
(54) Paesani, F.; Iuchi, S.; Voth, G. A. *J. Chem. Phys.* **2007**, *127*, 074506.
(55) *CRC Handbook of Chemistry and Physics*; CRC Press: Boca Raton, FL, 2013.
(56) Wagner, W.; Pruss, A. *J. Phys. Chem. Ref. Data* **2002**, *31*, 387−535.
(57) Krynicki, K.; Green, C. D.; Sawyer, D. W. *Faraday Discuss.* **1978**, *66*, 199−208.
(58) Rezus, Y. L. A.; Bakker, H. J. *J. Chem. Phys.* **2005**, *123*, 114502.
(59) Soper, A. K. *J. Chem. Phys.* **2000**, *258*, 121−137.
(60) Soper, A. K.; Benmore, C. J. *Phys. Rev. Lett.* **2008**, *101*, 065502.
(61) Skinner, L. B.; Huang, C. C.; Schlesinger, D.; Pettersson, L. G. M.; Nilsson, A.; Benmore, C. J. *J. Chem. Phys.* **2023**, *138*, 074506.
(62) Fanourgakis, G. S.; Xantheas, S. S. *J. Chem. Phys.* **2008**, *128*, 074506.
(63) Habershon, S.; Markland, T. E.; Manolopoulos, D. E. *J. Chem. Phys.* **2009**, *131*, 024501.
(64) Ceriotti, M.; Cuny, J.; Parrinello, M.; Manolopoulos, D. E. *Proc. Natl. Acad. Sci. U.S.A.* **2013**, *110*, 15591−15596.
(65) Grimme, S.; Antony, J.; Ehrlich, S.; Krieg, H. *J. Chem. Phys.* **2010**, *132*, 154104.
(66) Wang, L.; Ceriotti, M.; Markland, T. E. Private communication.
(67) Keutsch, F. N.; Saykally, R. J. *Proc. Natl. Acad. Sci. U.S.A.* **2001**, *98*, 10533−10540.